

Light Load Efficiency Boost Technique for Switched Tank Converters Based on Hybrid ZVS-ZCS Control

Jiawei Liang, Haoyu Wang

School of Information Science and Technology

ShanghaiTech University, Shanghai, China

Shanghai Engineering Research Center of Energy Efficient and Custom AI IC

wanghy@shanghaitech.edu.cn

Abstract—In data center applications, the low voltage load typically operates under light-load conditions. Hence, the light-load efficiency of the switched tank converter (STC) is crucial for energy saving. In this paper, a hybrid soft switching control scheme is proposed to improve the light-load efficiency of STC. The proposed control technique regulates the frequency and phase shift between wing-side switches and bridge-side switches such that the converter is tuned in either ZCS or ZVS mode. At heavy load, the large current and high switching frequency make the switching loss of ZVS mode more severe than that of ZCS mode. While at light load, switching loss in ZCS mode is fixed and significant compared with the negligible switching loss in ZVS mode. The proposed control technique enables ZCS mode at heavy load and ZVS mode under light load, respectively. Hence, high efficiency over a wide load range can be achieved. Two modes of steady-state circuit analysis are briefed and the simulation model is established to verify the analysis. A hardware prototype that converts 48 V to 12 V is designed and tested. The results demonstrate that the light load efficiency can be improved remarkably using the proposed technique.

Index Terms—light-load efficiency, switched-tank converter, zero current switching, zero voltage switching.

I. INTRODUCTION

Data center is becoming the critical infrastructure with the rapid development of 5G communication, big data, and scientific computing. It is predicted that the energy consumption of global data centers will reach 8% of total worldwide electric power consumption by 2030 [1]. However, the typical data center in enterprises only delivers 5% to 15% of its maximum computing output on average [2]. Moreover, more than 89% of the operation time has a rated power less than 10%. Namely, the power supply mainly operates under standby (idle) and light-load conditions [3]. Therefore, improving the light-load efficiency is critical for energy saving in data centers.

The latest power architecture in data center utilizes a 48 V distribution bus with voltage regulator modules (VRM). The two-stage structure is popular on the server motherboard. At the front end, a non-regulated converter is utilized to convert the 48 V to an intermediate voltage (e.g. 5 V-12 V), and the

back end employs a point-of-load (PoL) converter such as multiphase buck [4] to regulate the intermediate voltage to 1 V-1.8 V for terminal loads. Optimizing the design of the front-end non-regulated converter is very important to achieve high conversion efficiency and high power density.

Full bridge LLC resonant converters are widely used in the front end due to their zero voltage switching (ZVS) for primary-side MOSFETs and zero current switching (ZCS) for secondary-side diodes. Although LLC light-load efficiency can be improved by dynamic reconfiguration [5], large circulating current in the LLC transformer still exists. Moreover, the bulky transformer leads to bulky size and high power loss. To improve the power density, switched capacitor converter (SCC) based solutions are good candidates. Unfortunately, when the capacitors of traditional SCCs are reconfigured, the charge redistribution loss leads to harsh transient currents. Correspondingly, small inductors can be added into SCC to resonate with the corresponding capacitors, which facilitates a soft charging of capacitors. Furthermore, the SCC with small inductors can operate under either ZCS mode or ZVS mode. Since the terminal loads operate under low voltage and high current conditions, ZCS is more beneficial than ZVS in data center applications. A popular switched capacitor topology with small inductors called switched tank converter (STC) is proposed in [6]. For STC, it can achieve ZCS operation for all MOSFETs with easy open-loop control. However, the switching losses caused by the output capacitance of MOSFET dominate the total loss at light load in the ZCS operation, which drastically reduces the efficiency.

To improve the light-load efficiency caused by the switch output capacitance-related switching losses, this paper proposes a new control technique for STC. The proposed technique regulates the frequency and phase shift between wing-side switches and bridge-side switches so that the converter operates in either ZCS or ZVS mode to optimize the efficiency under different loads. Generally, the switching frequency of ZVS-type STC [7], [8] is much higher than the resonant frequency in the resonant tank, so the frequency-dependent losses are considerable. Moreover, ZVS turn-off is significant under low voltage and large current conditions compared with

This work was supported in part by the National Natural Science Foundation of China under Grant 52077140, and in part by the Shanghai Rising Star Program under Grant 20QA1406700.

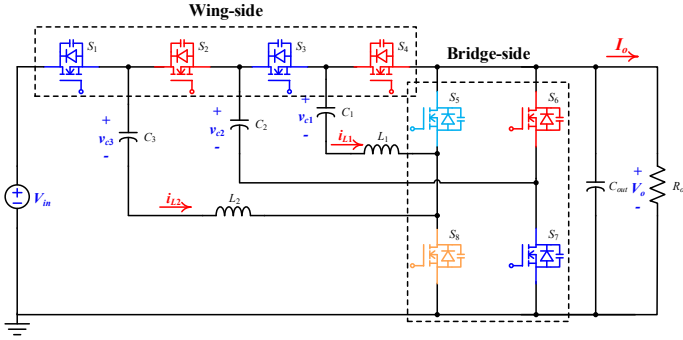


Fig. 1. Schematic of the 4-to-1 STC Converter based on merged H-bridge.

the negligible switching loss in ZCS mode. Consequently, ZCS with fixed switching losses and a lower switching frequency is more competitive than ZVS. Nevertheless, the reduced current makes the “negligible” switching loss of ZCS mode non-negligible at light load. Correspondingly, the abandoned ZVS mode, which can eliminate the switching loss caused by the switch output capacitance, is reconsidered. The basic converter operations of ZCS and ZVS are analyzed and the simulation of a merged H-bridge-based STC converter has been carried out to verify the concept. A 48 V-to-12 V, fixed ratio converter prototype is built and tested to verify the theoretical analysis.

The rest of the paper is organized as follows. Section II introduces the soft switching control scheme of the merged H-bridge-based STC converter along with its steady-state operation and presents the steady-state analysis of key waveforms in ZCS and ZVS modes. Moreover, the power loss analysis is depicted. Simulation is carried out with the PSIM platform in Section III. A 48 V input to 12 V output hardware prototype is developed and the experimental results are demonstrated. Finally, this paper concludes in Section IV.

II. ANALYSIS OF PROPOSED ZVS-ZCS CONTROL SCHEME

The schematic of the merged H-bridge-based STC converter with a 4:1 conversion ratio is shown in Fig. 1. It consists of two LC resonant tanks and a non-resonant capacitor C_{nr} (C_2), where each resonant tank contains a resonant capacitor C_r (C_1 or C_3) and a resonant inductor L_r (L_1 or L_3). Moreover, there are four color switches with two pairs of complementary gate signals. The gate signals of dark blue switches and red switches are one pair, while the signals of the light blue switch and orange switch are the other pair. Depending on the frequency and phase shift between two pairs of gate signals, the converter can operate in either ZCS or ZVS mode with a 4 to 1 conversion ratio.

A. ZCS Mode

The STC operating in ZCS mode has been comprehensively discussed in [9]. Only a pair of 50% duty cycle complementary gate signals with certain deadband are utilized to drive two groups of switches which are the odd-numbered switches ($S_{1,3,5,7}$) and even-numbered switches ($S_{2,4,6,8}$). Without considering the deadband, the converter can achieve

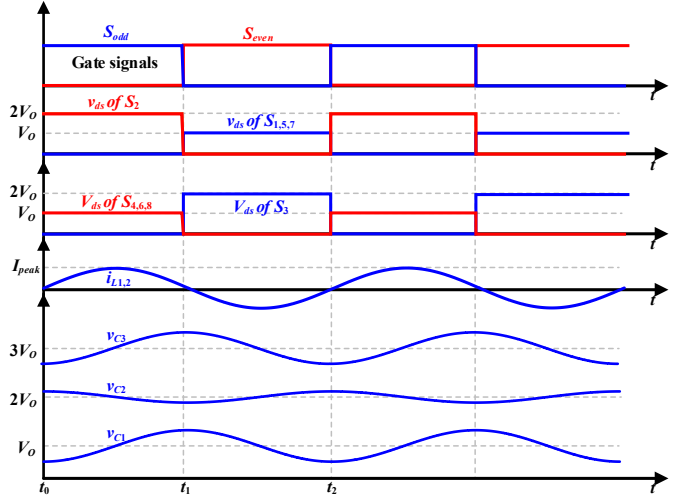


Fig. 2. Ideal switching waveforms of ZCS mode at steady-state.

ZCS operation when the switching frequency is matched to the resonant frequency,

$$f_s = f_r = \frac{1}{2\pi\sqrt{L_r C_r}} \quad (1)$$

where f_s , f_r , L_r , and C_r are the switching frequency, resonant frequency, resonant inductance, and resonant capacitance in the resonant tank, respectively. Practically, many factors, such as the tolerance of resonant components or the parasitic components, can cause the mismatch of the resonant parameters in different resonant loops. Once there is a trivial error in the resonant parameters, ZCS will be lost. The general method mentioned in [9], [10] is to add a small deadband during the switching transition to reset all inductor currents, so the actual switching frequency is slightly less than the resonant frequency to ensure ZCS operation.

Fig. 2 illustrates the ideal waveforms during steady state. The capacitor voltages satisfy $V_n = nV_o$ ($n=1,2,3$). The voltage stresses of the switches $S_{1,3,5,7}$ are V_o and the switches $S_{2,3}$ have the voltage stress $2V_o$. The low voltage stress of switches is one of the advantages of switched capacitor-based converters.

B. ZVS Mode

The proposed control technique to achieve ZVS is based on the phase-shift control method [11] which is generally used to regulate the voltage conversion ratio of the switched-capacitor-based resonant converters. The phase shift between two pairs of 50% duty cycle complementary gate signals is set to the minimum required deadband of ZVS so that the conversion ratio is close to the nominal conversion ratio (eg. 4:1). The ideal waveforms of the inductor voltage and current are presented in Fig. 3. The operation modes neglecting the dead time are analyzed as follows:

1) *Mode I* ($t_0 - t_1$): The dark blue switches $S_{1,3,7}$ and the orange switch S_8 are on, the red switches $S_{2,4,6}$ and light blue

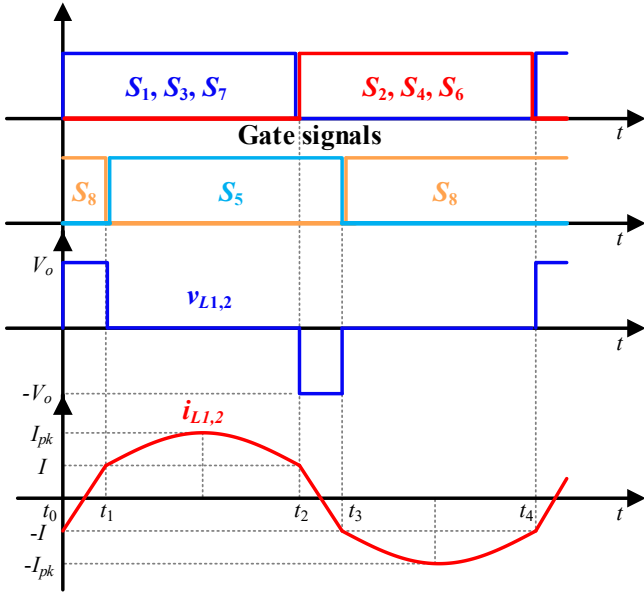


Fig. 3. Ideal switching waveforms of ZVS mode at steady-state.

switch S_5 are off. The voltage across the inductor is V_o , and the inductor current increases linearly.

2) *Mode II* ($t_1 - t_2$): At t_1 , the light blue switch S_5 turns on, the orange switch S_8 turns off. The capacitors $C_{1,3}$ resonate with the inductors $L_{1,2}$, respectively, so the inductor current is sinusoidal.

3) *Mode III* ($t_2 - t_3$): The red switches $S_{2,4,6}$ and the light blue switch S_5 are on, the dark blue switches $S_{1,3,7}$ and orange switch S_8 are off. The voltage across the inductor is $-V_o$, and the inductor current decreases linearly.

4) *Mode IV* ($t_3 - t_4$): The orange switch S_8 turns on and the light blue switch S_5 turns off at t_3 . The inductor current becomes sinusoidal again since the capacitors $C_{1,3}$ resonate with the inductors $L_{1,2}$.

Assuming that the inductor current and capacitor voltage are constant during the short deadtime, the detailed switching waveforms with deadtime are illustrated in Fig. 4. To analyze the ZVS process, the deadtime at t_2 , as an example, can be divided into two segments:

- $[t_a, t_b]$: At t_a , the dark blue switches turn off. The inductor currents begin to charge and discharge the output capacitors C_{oss1-4} of all wing-side MOSFETs until the output capacitor C_{oss4} of S_4 has been fully discharged and its body diode conducts. Hence, S_4 satisfies the ZVS turn-on condition.
- $[t_b, t_c]$: In this interval, the inductor current i_{L2} continues to charge and discharge the output capacitors $C_{oss1,2}$ of $S_{1,2}$ until the body diode of S_2 is on. It seems that S_2 achieves ZVS, but a quarter of the energy stored in C_{oss2} which transfers between C_{oss1} and C_{oss2} will be dissipated when the red switches turn on at t_c . Based on this, S_2 is considered that achieve partial ZVS turn-on, and

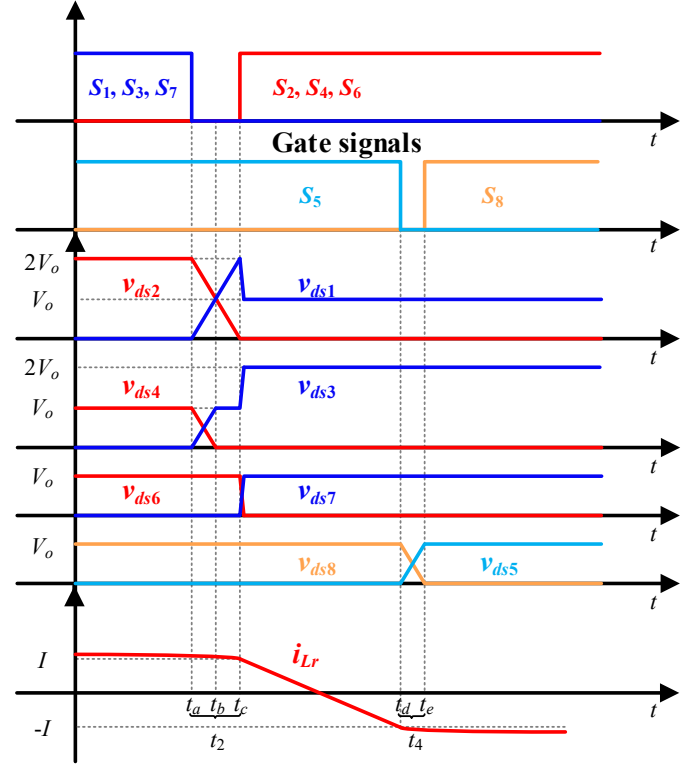


Fig. 4. Detailed ZVS processes of the converter considering switching transitions during dead times.

the deadtime ends at any time within this interval have the identical switching loss which means the accurate deadtime calculation is not necessary.

For the STC converter shown in Fig. 1, four switches ($S_{1,4,5,8}$) can achieve ZVS turn-on, two switches ($S_{2,3}$) can achieve partial ZVS turn-on, and two switches ($S_{6,7}$) operate in hard switching mode. The major ZVS condition is that the inductor current can fully absorb the energy stored in the output capacitor of MOSFETs,

$$L_r I^2 \geq C_{oss} V_{ds}^2 \quad (2)$$

where L_r , I , C_{oss} , and V_{ds} are resonant inductance, inductor current at switching transition, MOSFET output capacitance, and the drain-to-source voltage of MOSFET, respectively.

C. Switching Loss Analysis

The switching loss in ZCS mode is only caused by the output capacitor since all of the switches operate with ZCS. The output capacitor of MOSFETs is charged during the turn-off transition, and these charges will be dissipated within the MOSFETs when the MOSFETs turn on. Thus, the switching loss can be calculated as

$$P_{sw_ZCS} = \frac{1}{2} C_{oss} V_{ds}^2 f_s \quad (3)$$

In ZVS mode, ZVS switches only have the turn-off switching loss, partial ZVS switches have both turn-on and turn-off losses with half of the drain-to-source voltage, and the

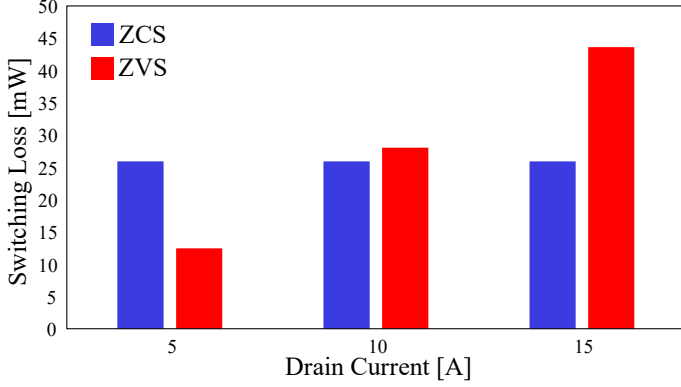


Fig. 5. Switching losses of MOSFET operating in ZCS and ZVS modes.

switching losses of hard-switched switches include turn-on and turn-off losses. A simple analytical switching loss model is depicted in Vishay's application note [12], and the turn-on switching loss P_{sw_on} and the turn-off switching loss P_{sw_off} can be expressed as,

$$\begin{cases} P_{sw_on} = \frac{1}{2} V_{ds} I_d f_s t_{on} \\ P_{sw_off} = \frac{1}{2} V_{ds} I_d f_s t_{off} \end{cases} \quad (4)$$

and

$$\begin{cases} t_{on} = R_G C_{iss} \ln \frac{V_{gs} - V_{th}}{V_{gs} - V_{gp}} + R_G C_{gd} \frac{V_{ds}}{V_{gs} - V_{gp}} \\ t_{off} = R_G C_{iss} \ln \frac{V_{gp}}{V_{th}} + R_G \frac{\Delta Q_{gd} V_{ds}}{\Delta V_{ds} V_{gp}} \end{cases} \quad (5)$$

where R_G is the effective total gate resistance, C_{iss} is the input capacitance, V_{gs} is the gate source voltage, V_{gp} is the gate plateau voltage, V_{th} is the gate threshold voltage, C_{gd} is the gate to drain capacitance, and Q_{gd} is the gate to drain charge. These parameters can be obtained from the datasheet of MOSFET.

Fig. 5 compares the switching losses at different drain currents for a MOSFET operating in ZCS and ZVS modes. The switching losses caused by the output capacitor in ZCS mode are fixed since it is independent of drain current. By contrast, the variable switching losses in ZVS mode increase along with the increase of drain current. Generally, the switching losses in ZVS mode only are considered to have only the turn-off losses. Thus, the switching losses in ZVS mode are negligible due to the low turn-off losses of MOSFET at a low current. This fact makes the ZVS-ZCS hybrid control scheme potential to reduce the losses under different loads. Therefore, the proposed control technique controls the converter operating in ZVS mode under light load and change from ZVS mode to ZCS mode under heavy load to improve the overall efficiency.

III. SIMULATION AND EXPERIMENTAL RESULTS

A. Simulation Results

To validate the operating principle, the merged H-bridge-based STC converter with a 4:1 conversion ratio is simulated in PSIM. Table I lists the key parameters. The simulation results

TABLE I
PARAMETERS OF THE 4:1 STC CONVERTER

Symbol	Meaning	Value	
		ZCS mode	ZVS mode
V_{in}	Input Voltage	48 V	
V_o	Output Voltage	12 V	
C_r	Resonant Capacitor	1.76 μ F	
C_{nr}	Non-Resonant Capacitor	120 μ F	
L_r	Resonant Inductor	200 nH	
f_r	Resonant Frequency	268 kHz	
f_s	Switching Frequency	258 kHz	282 kHz
t_d	Dead Time	50 ns	
ϕ	Phase Shift	0°	4.83°

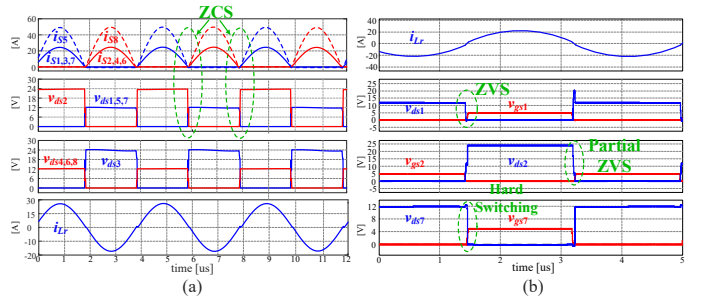


Fig. 6. Simulation results: (a) voltage/current waveforms in ZCS mode; (b) voltage/current waveforms in ZVS mode.

of ZCS mode are shown in Fig. 6(a), and the voltage stresses of MOSFETs are V_o ($S_{1,4-8}$) and $2V_o$ ($S_{2,3}$), respectively. When the switching frequency is close to the resonant frequency, the resonant current reaches zero at the switch transitions which means the switches can achieve ZCS operation. Fig. 6(b) shows the waveforms of inductor currents and V_{ds} of three-types switches (ZVS, partial ZVS, and hard switching), among which S_1 can achieve ZVS turn-on, S_2 can achieve partial ZVS turn-on, S_7 operates in hard switching mode.

B. Experimental Results

A hardware prototype based on the merged H-bridge STC converter has been built to verify the proposed control scheme. The prototype operates with 48 V input and 12 V output. DSP TMS320F28379 is used as the digital controller to generate the pulsewidth modulation signals, and the load uses the Chroma electric load as the variable resistor to handle different output currents. The components used in this prototype are listed in Table II. The experimental results are captured in Fig. 7. Fig. 7(a) and 7(b) show the switching waveforms of ZVS, partial ZVS and hard switching, and the waveforms of inductor current in ZVS mode. In Fig. 7(c), the resonant currents are almost identical and reach zero at the switching transition, which indicates ZCS operation is achieved. The voltage stresses of $S_{3,4}$ are 24 V ($2V_o$) and 12 V (V_o), respectively. To optimize the soft switching control scheme, the efficiency of ZCS mode and ZVS mode are measured and the result is shown in Fig. 7(d). When the output power is lower than 100 W, the ZVS mode shows a higher light-load efficiency. The peak efficiency is 98.2% at 52 W output

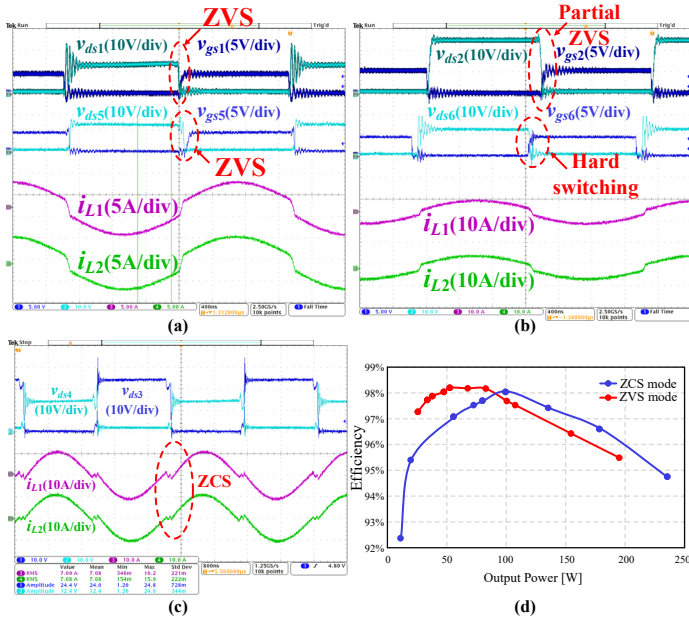


Fig. 7. Experimental Results: (a-b) the drain to source and gate to source voltage waveforms of $S_{1,2,5,6}$, and the inductor current waveforms of $L_{1,2}$ in ZVS mode; (c) the drain to source voltage waveforms of $S_{3,4}$, and the inductor current waveforms of $L_{1,2}$ in ZCS mode and ZVS mode; (d) the experimental efficiency in ZCS mode and ZVS mode.

TABLE II
COMPONENTS SELECTION

Components	Part number
MOSFET	BSZ013NE2LS5I (25 V, 1.3 mΩ)
Resonant Capacitor	C1812C224J5GAC
Non-Resonant Capacitor	C1210C106K5RACTU
Resonant Inductor	SLC7649S-101KLC
Gate Driver	LM5113SD
Digital Isolator	Si8620BB
Isolated Power	B0505XT-1WR3

and the overall light-load efficiency can maintain above 97%. As the output power increases, the operation mode changes from ZVS mode to ZCS mode since the ZCS mode with fixed switching loss is more beneficial than ZVS mode, resulting in a significant improvement in the overall efficiency.

IV. CONCLUSION

In this paper, a hybrid ZVS-ZCS control technique is proposed to improve the light-load efficiency of the merged H-4 bridge-based STC converter. It controls the converter to operate in ZVS mode under light load to reduce the switching loss caused by the switch output capacitance, and changes from ZVS mode to ZCS mode to eliminate the increase in switching loss due to large current, thereby improving the overall efficiency. The steady-state analysis of important waveforms in ZCS mode and ZVS mode and the switching loss analysis are discussed. A 48 V input to 12 V output hardware prototype is designed and tested. The simulation and experimental results validate the analysis of the proposed control scheme. In the future, a more accurate switching loss

model will be built to further analyze the pros and cons between ZVS and ZCS.

REFERENCES

- [1] Supermicro, "Data center & the environment: 2021 report on the state of the green data center," 2021. [Online]. Available: [https://marketing-email.supermicro.com/hubfs/PDFs/DataCenters&theEnvironmentReport2021CondensedV1%20\(1\).pdf](https://marketing-email.supermicro.com/hubfs/PDFs/DataCenters&theEnvironmentReport2021CondensedV1%20(1).pdf)
- [2] J. Koomey, J. Taylor *et al.*, "New data supports finding that 30 percent of servers are 'comatose', indicating that nearly a third of capital in enterprise data centers is wasted," *TSO logic*, Jun. 2015.
- [3] "Energy-efficient performance on the client," *Intel White Paper*, Santa Clara, CA, Sept. 2007. [Online]. Available: http://book.itep.ru/depository/green_computing/EEP_whitepaper.pdf
- [4] M. Esteki, B. Poorali, E. Adib, and H. Farzanehfard, "Interleaved buck converter with continuous input current, extremely low output current ripple, low switching losses, and improved step-down conversion ratio," *IEEE Trans. Ind. Electron.*, vol. 62, no. 8, pp. 4769–4776, Aug. 2015.
- [5] C. Fei, M. H. Ahmed, F. C. Lee, and Q. Li, "Two-stage 48 v-12 v/6 v-1.8 v voltage regulator module with dynamic bus voltage control for light-load efficiency improvement," *IEEE Trans. Power Electron.*, vol. 32, no. 7, pp. 5628–5636, Jul. 2017.
- [6] S. Jiang, S. Saggini, C. Nan, X. Li, C. Chung, and M. Yazdani, "Switched tank converters," *IEEE Trans. Power Electron.*, vol. 34, no. 6, pp. 5048–5062, Jun. 2019.
- [7] H. Setiadi and H. Fujita, "An asymmetric control method for switched-capacitor-based resonant converters," *IEEE Trans. Power Electron.*, Sept. 2021.
- [8] S. Khatua, D. Kastha, and S. Kapat, "A dual active bridge derived hybrid switched capacitor converter based two-stage 48 v vrm," *IEEE Trans. Power Electron.*, vol. 36, no. 7, pp. 7986–7999, Jul. 2021.
- [9] Y. Li, X. Lyu, D. Cao, S. Jiang, and C. Nan, "A 98.55% efficiency switched-tank converter for data center application," *IEEE Trans. Ind. Appl.*, vol. 54, no. 6, pp. 6205–6222, Nov.-Dec. 2018.
- [10] J. C. Rosas-Caro, J. C. Mayo-Maldonado, F. Mancilla-David, A. Valderrabano-Gonzalez, and F. B. Carbajal, "Single-inductor resonant switched capacitor voltage multiplier with safe commutation," *IET Power Electron.*, vol. 8, no. 4, pp. 507–516, Apr. 2015.
- [11] K. Sano and H. Fujita, "Performance of a high-efficiency switched-capacitor-based resonant converter with phase-shift control," *IEEE Trans. Power Electron.*, vol. 26, no. 2, pp. 344–354, Feb. 2011.
- [12] J. Brown, "Power mosfet basics: Understanding gate charge and using it to assess switching performance," *Vishay Siliconix, AN608*, vol. 153, Dec. 2004.